ZW sex-chromosome evolution and contagious parthenogenesis in Artemia brine shrimp

Marwan Elkrewi[1#], Uladzislava Khauratovich[1,2#], Melissa A. Toups[1,3#], Vincent Kiplangat Bett[1], Andrea Mrnjavac[1], Ariana Macon[1], Christelle Fraisse[1,4], Luca Sax[1,5], Ann Kathrin Huylmans[1,6], Francisco Hontoria[7], Beatriz Vicoso[1@]

[1] Institute of Science and Technology Austria, Klosterneuburg, 3400, Austria

[2] Department of Chromosome Biology, Max Perutz Labs, University of Vienna, 1030, Austria

[3] Department of Life and Environmental Sciences, Faculty of Science and Technology, Bournemouth University, BH12 5BB, UK

[4] CNRS, Univ. Lille, UMR 8198 – Evo-Eco-Paleo, F-59000 Lille, France

[5] Lewis and Clark College, Portland, OR 97219, USA

[6] Institute of Organismic and Molecular Evolution, Johannes Guttenberg Universität Mainz, Mainz, 55122, Germany

[7] Instituto de Acuicultura de Torre de la Sal (IATS-CSIC), Ribera de Cabanes, 12595, Spain

[@] bvicoso@ist.ac.at

[#] These authors contributed equally to this work.

Keywords: sex chromosome; female heterogamety; asexuality; dosage compensation

Abstract

Eurasian brine shrimp (genus *Artemia*) have closely related sexual and asexual lineages of parthenogenetic females, which produce rare males at low frequencies. Although they are known to have ZW chromosomes, these are not well characterized, and it is unclear whether they are shared across the clade. Furthermore, the underlying genetic architecture of the transmission of asexuality, which can occur when rare males mate with closely related sexual females, is not well understood. We produced a chromosome-level assembly for the sexual Eurasian species *A. sinica* and characterized in detail the pair of sex chromosomes of this species. We combined this new assembly with short-read genomic data for the sexual species *A. sp. Kazakhstan* and several asexual lineages of *A. parthenogenetica,* allowing us to perform an in-depth characterization of sex-chromosome evolution across the genus. We identified a small differentiated region of the ZW pair that is shared by all sexual and asexual lineages, supporting the shared ancestry of the sex chromosomes. We also inferred that recombination suppression has spread to larger sections of the chromosome independently in the American and Eurasian lineages. Finally, we took advantage of a rare male, which we backcrossed to sexual females, to explore the genetic basis of asexuality. Our results suggest that parthenogenesis is likely partly controlled by a locus on the Z chromosome, highlighting the interplay between sex determination and asexuality.

Introduction

The diversity of reproductive and sex-determining systems has long puzzled evolutionary biologists (Bachtrog *et al.* 2014; Pennell *et al.* 2018; Picard *et al.* 2021). When separate sexes are present, the development of males and females can be controlled by environmental factors or through the presence of sex-determining loci (Beukeboom and Perrin 2014; Bachtrog *et al.* 2014). These sex determining loci are typically carried by specialized “sex chromosomes”, such as the X and Y chromosomes of mammals. Sex chromosomes initially arise from standard pairs

of autosomes, but can progressively stop recombining over much of their length, ultimately resulting in genetic and morphological differentiation (Charlesworth *et al.* 2005; Wright *et al.* 2016). Each segment of the sex chromosome pair that stopped recombining at a given timepoint is referred to as a "stratum", and strata of different ages are often found on the same pair of sex chromosomes (Lahn and Page 1999; Handley *et al.* 2004). The Y chromosome stops recombining altogether after XY recombination suppression and eventually degenerates, i.e., it accumulates deleterious mutations and can lose many or even all of its genes (Bachtrog 2013). This gene loss leads to dosage deficits in males, since many X-linked genes become single-copy. Mechanisms of dosage compensation often target the X-chromosome and regulate its expression, thereby reestablishing optimal dosage balance of genes across the genome (Charlesworth 1978; Straub and Becker 2007; Vicoso and Bachtrog 2009; Disteche 2016). Alternatively, both the silencing of Y-linked genes and compensation of X-linked genes may arise concurrently as a result of runaway regulatory divergence that sets up and reinforces the predominance of X over Y expression (Lenormand *et al.* 2020; Lenormand and Roze 2022). Much of our understanding of these processes has come from studying the ancient XY systems of traditional model organisms such as mice and fruit flies. Despite the recent characterization of young sex chromosomes in many nonmodel species (Charlesworth 2019), many questions remain about the earlier stages of sex-chromosome divergence. For example, what molecular mechanisms and selective pressures drive the initial loss of recombination between sex chromosomes (Ponnikas *et al.* 2018)? Similarly, female-heterogametic species (i.e., females are ZW, males are ZZ) have remained relatively understudied, as they are not found in any of the main model organisms. While parallels exist between the evolution of XY and ZW pairs, such as the progressive loss of recombination and subsequent degradation of the Y/W-chromosomes (Ellegren 2011; Vicoso *et al.* 2013; Zhou *et al.* 2014; Picard *et al.* 2018; Sigeman *et al.* 2021), some aspects of their evolution seem to differ. In particular, dosage compensation of Z-chromosomes is often limited to a few dosage-sensitive genes (i.e., it works gene-by-gene, as

opposed to the chromosome-wide mechanisms found in many XY species, (Mank 2013; Rovatsos and Kratochvíl 2021)). These discrepancies may have to do with systematic differences in selection and mutation between males and females (Vicoso and Bachtrog 2009; Ellegren 2011; Mullon *et al.* 2015), or may simply be a coincidence due to the few ZW systems characterized in detail at the molecular level (Rovatsos and Kratochvíl 2021).

Although the prevalence of sexual reproduction suggests that it offers long-term advantages, asexual lineages are found in many clades and successfully inhabit a variety of ecological niches (Toman and Flegr 2018). Transitions from sexual to asexual reproduction are frequent (Neiman et al., 2014), and can involve a diversity of mechanisms that disrupt meiosis, such as novel mutations, hybridization of closely related lineages, and polyploidization (Neiman *et al.* 2014). Asexuality can evolve from any ancestral sex-determining system, including in species with differentiated sex chromosomes, (e.g., Schwander and Crespi 2009; Jaquiéry *et al.* 2014; Mignerot *et al.* 2019), and understanding the mechanisms underlying these transitions has been a key goal of the field.

In many asexual lineages, males are occasionally produced, and can fertilize closely related sexual females, which then give rise to new asexual lineages (“contagious parthenogenesis”). These crosses have facilitated the use of traditional genetic approaches for understanding the genetic architecture of asexuality (Jaquiéry *et al.* 2014). Transitions from sexual to asexual reproduction have primarily been studied in animal species where both sexual reproduction and parthenogenesis were ancestrally part of the life cycle, either in the form of cyclical parthenogenesis or haplodiploidy (Neiman *et al.* 2014). In this case, the loss of sexual reproduction and consequent obligatory parthenogenesis is often controlled by one or only a few loci (Lynch *et al.* 2008; Sandrock and Vorburger 2011; Eads *et al.* 2012; Jaquiéry *et al.* 2014; Aumer *et al.* 2017; Yagound *et al.* 2020). In the pea aphid, the locus controlling asexuality is found on the X-chromosome (Jaquiéry *et al.* 2014), and a locus of large effect on parthenogenesis was also found on the UV sex chromosome pair of brown algae *Ectocarpus*

(Mignerot *et al.* 2019), raising interesting questions about the interplay between the ancestral sex-determining system and contagious parthenogenesis. One direct link between the two phenomena is that when asexuals are derived from an ancestral XX/XY or haplodiploid sex-determination systems, rare males can be formed through the loss of an X-chromosome (Kampfraath *et al.* 2020) or through accidental production of haploid individuals during automixis (Sandrock and Vorburger 2011). Less is known about the creation of rare males when the ancestral sex-determination system was female-heterogamety. More generally, it is unclear if sex chromosomes are a prime spot for the location of genes regulating asexual reproduction, since very few transitions have been characterized in organisms with sex chromosomes.

Brine shrimp of the genus *Artemia* have both asexual and sexual species (Abatzopoulos 2018), as well as ZW sex chromosomes with putative ancient and recent strata (Bowen 1963; De Vos *et al.* 2013; Accioly *et al.* 2015; Huylmans *et al.* 2019), making them an ideal model for addressing many of these questions. While all American species are sexual, the Eurasian clade consists of a few sexual species (including *A. sinica, A. sp. Kazakhstan* and *A. urmiana*) and of various asexual lineages (collectively refered to as *A. parthenogenetica*, and further referred to by their location of origin) (Van Stappen 2002; Maccari *et al.* 2013b). Asexuals vary in ploidy, but only diploid lineages are considered here (Maccari *et al.* 2013b). Originally thought of as ancient, these lineages turned out to have arisen recently through hybridization between asexual lineages and individuals from, or closely related to, *A. sp. Kazakhstan* (Baxevanis *et al.* 2006; Maccari *et al.* 2013b; Rode *et al.* 2022). In *Artemia*, such contagious parthenogenesis can occur through the production of rare males by asexual lineages, which can fertilize closely related sexual females (Maccari *et al.* 2013a; Abatzopoulos 2018). Furthermore, asexual females can mate with males of sexual species and produce a minority of offspring sexually (Boyer *et al.* 2021). The ZW pair of *Artemia* has been mostly studied in the American species *A. franciscana* (Bowen 1963; Parraguez *et al.* 2009; De Vos *et al.* 2013; Accioly *et al.* 2015). Both a small differentiated region and a non-recombining but largely undifferentiated region were

detected, making it an interesting system to understand the first steps leading to ZW divergence (Huylmans *et al.* 2019). Gene expression in the differentiated region appears to be fully balanced between males and females, but there was limited power to detect changes due to the fragmented nature of the genome (Huylmans *et al.* 2019). Eurasian lineages also carry a ZW pair (Haag *et al.* 2017), but whether the same chromosome is used for sex determination accross the clade in not known. Because *A. parthenogenetica* reproduce through central fusion automixis (Nougué *et al.* 2015), a modified form of meiosis, which allows for loss of heterozygosity when recombination between chromosomes occurs, rare recombination events between the Z and W (which replace part of the W with its Z-linked homologous region) can lead to the creation of rare males (Nougué *et al.* 2015; Boyer *et al.* 2022). Finally, the genetic mechanisms behind asexuality, and whether the sex chromosomes play any further role in its evolution, have not yet been explored in detail.

Here, we develop several genomic resources for *Artemia* lineages, including the first chromosome-level assembly for the *Artemia* genus (*A. sinica*), as well as short-read genomic data for *A. sp. Kazakhstan* and several lineages of *A. parthenogenetica* (see Fig. S1 for a phylogeny of the lineages). Using these data, we are able to provide an in-depth characterization of sex-chromosome evolution across the genus, including identifying an ancient region shared with the American species *A. franciscana*. Finally, we find evidence that asexuality is likely partly controlled by a locus on the Z chromosome - a first in a ZW sex chromosome system.

Materials and methods

Sampling and DNA extractions

Cysts from *A. sinica* (originally from Tanggu salterns, PR China), *A. sp. Kazakhstan* (originally from an unknown location in Kazakhstan), and two lineages of *A. parthenogenetica* (from Lake Aibi (PR China) and from Lake Urmia (Iran)) were obtained from the Instituto de

Acuicultura de Torre de la Sal (C.S.I.C.) Artemia cyst collection in Spain, as described in (Huylmans *et al.* 2021). Cysts were hatched under 30 g/L salinity and grown to adulthood under 60 g/L salinity. Some of these F0 individuals were used directly for DNA extractions with the Qiagen DNeasy Blood & Tissue kit. We also set up iso-female lines in *A. sinica* and *A. sp. Kazakhstan*, and subjected them to 6 generations of sib-sib mating to reduce the amount of heterozygosity. Male and female individuals from *A. sinica* and *A. sp. Kazakhstan* inbred iso-female lines were used individually for DNA extractions with Qiagen DNeasy Blood & Tissue kit. Furthermore, 20 males and 17 females of *A. sinica* (also from the inbred iso-female line) were pooled and high molecular weight DNA was extracted using the Qiagen Genomic-tip 20/G kit.

DNA short and long read sequencing

PacBio libraries were prepared and sequenced at the Vienna Biocenter Sequencing facility for the male and female *A. sinica* high molecular weight DNA. All other DNA samples were used for Illumina paired-end sequencing. Libraries were prepared and sequenced at the Vienna Biocenter Sequencing Facility. Finally, 1 male was frozen and provided to the sequencing facility for Hi-C library preparation and Illumina sequencing on a NovaSeq machine. The final list of samples, as well as the parts of the analysis that they were used in, are listed in Table S1.

Genome assemblies

The male PacBio reads were assembled using two different genome assemblers: Flye (v.2.7.1, Kolmogorov *et al.* 2019) and Miniasm (0.3-r179, minimap2 2.18-r1028-dirty was used for mapping and the consensus was generated using Racon v1.4.22)(Li 2016; Vaser *et al.* 2017). The Flye assembly was polished using male *Artemia sinica* short genomic reads (trimmed with the Trimmomatic package, Bolger *et al.* 2014), and the Miniasm assembly was polished using the same male short reads using the wtpoa-cns tool from wtdbg2 (version 2.5, Ruan and Li 2020). The two assemblies were then merged using quickmerge (version 0.3,

Chakraborty *et al.* 2016) with the Miniasm assembly as the query and the Flye assembly as the reference. The resulting assembly was purged based on the male pacbio read depth to remove duplicates and contig overlaps using the purge_dups program (version 1.2.5, Guan *et al.* 2020).

To scaffold the assembly into pseudo-chromosomes, the PCR duplicates were first removed from the Hi-C data using the clumpify.sh script from the BBMap package (Bushnell 2014), and the Hi-C reads were then mapped to the genome assembly using the Arima mapping pipeline with MAPQ 5 (Arima Genomics 2021) and then scaffolded using the YaHS tool (pre-release of version 1.1, Zhou *et al.* 2022). The contact maps were visualized and manually edited on Juicebox (version 1.11.08, Robinson *et al.* 2018) to generate the final chromosome-level assembly.

The female *Artemia sinica* genome was assembled from female PacBio reads using Flye (version 2.7.1), and it was not polished to avoid collapsing the Z and the W scaffolds. To identify putative W scaffolds, short genomic reads from two *A. sinica* males and two females were mapped to the female assembly using Bowtie2 (Langmead and Salzberg 2012). We then counted how many male and female reads mapped to each scaffold, after filtering for alignments without mismatches (by selecting only mapped reads with the CIGAR string "NM:i:0"). The female-specific k-mers inferred to obtain W-specific transcripts (section "Identification of candidate W-genes with k-mer analysis" below) were similarly mapped to each scaffold with Bowtie2 and counted. Scaffolds which had more than 5 female-specific k-mers, and more perfect matches in females than in males (male/(male+female)<=0.3) were considered candidates W-derived scaffolds, and are highlighted in orange in Fig. S2.

The *Artemia sp. Kazakhstan* genome was assembled from two male short read libraries with Megahit (v1.1.4, Li *et al.* 2015) and then scaffolded using SOAPdenovo-fusion (SOAPdenovo2 version 2.04, Luo *et al.* 2012).

BUSCO (version 5.2.2, Manni *et al.* 2021) was used to assess the completeness of the genomes generated in this study and the two previously published *Artemia franciscana* genomes in the genome mode with the arthropoda dataset (arthropoda_odb10).

Estimation of genomic coverage

The short genomic reads were mapped to the genome using bowtie2 (version 2.4.4, Langmead and Salzberg 2012). The uniquely mapped reads were then extracted from the output sam files using (grep -vw "XS:i"). SOAP.coverage (version 2.7.7, Luo *et al.* 2012) was then used to calculate the coverage for each library either using 10000 bp windows (*A. sinica*) or per scaffold (other species).

Mapping of *A. franciscana* markers to the *A. sinica* genome

The sequences of the *A. franciscana* SLAF markers were obtained from Han *et al.* (2021), and the left and right pairs of each marker were mapped to the *Artemia sinica* male genome separately using pblat (Wang and Kong 2019). Only the mapping location with the largest match score was kept for each marker.

Mapping of the *A. franciscana* and *A. sp. Kazakhstan* genomes to the new *A. sinica* assembly

We aligned the *A. sinica* published transcriptome (Huylmans *et al.* 2021) to both the *A. franciscana* and to the *A. sp Kazakhstan* genomic scaffolds using blat (Standalone BLAT v. 36x2, Kent 2002). For each transcript, we kept only the mapping location with the highest score in each genome (using the customized script 1-besthitblat.pl). When multiple transcripts overlapped by more than 20bps on the genome, only the transcript with the highest mapping score was kept (2-redremov_blat_v2.pl). We then used the location of the transcripts on the *Artemia sinica* genome to infer the location of the *A. franciscana* and *A. sp. Kazakhstan*

scaffolds based on the transcripts they carried (AssignScaffoldLocation.pl). This script uses a majority rule to assign each scaffold to a chromosome, and then the mean location of genes on that scaffold to infer its final coordinate on the chromosome. All scripts are available on our git page.

F_{ST} between male and female populations

RNA-seq reads from 10 pooled *A. sinica* males and 10 pooled *A. sinica* females (from Huylmans et al, 2021), sampled from head, thorax and gonads, were trimmed with Trimmomatic (Bolger *et al.* 2014) and pooled by sex, and mapped separately to the male *A.sinica* reference genome using STAR (Dobin *et al.* 2013) with default parameters.

The resulting alignments with MAPQ score lower than 20 were filtered out and the remaining alignments were sorted using samtools view and sort functions (Li *et al.* 2009). Next, a pileup file of male and female alignments was produced using the samtools-mpileup function. Finally, we used scripts from the Popoolation2 package (Kofler *et al.* 2011) to calculate F_{ST}. The mpileup file was reformatted with the Popoolation2 mpileup2sync.pl script, and the resulting synchronized file was used as an input for fst-sliding.pl script. F_{ST} between male and female populations was calculated for windows of 1000 nucleotides, using the fst-sliding.pl script with following options --suppress-noninformative --min-count 3 --min-coverage 10 --max-coverage 200 --min-covered-fraction 0.5 --window-size 1000 --step-size 1000 --pool-size 10.

We applied the same pipeline to estimate male:female F_{ST} using head and gonad RNA-seq samples obtained from 10 males and 10 females of *A. franciscana* (from Huylmans et *al.*, 2019). The resulting F_{ST} values were plotted based on the inferred location of the genomic scaffolds along the *A. franciscana* chromosomes (section “Mapping of the *A. franciscana* and *A. sp. Kazakhstan* genomes to the new *A. sinica* assembly”)**.**

Strata identification

ZW strata were identified based on the *A. sinica* coverage and F_{ST} analyses. First, we detected differentiated regions as any region where the Log2(female/male coverage) dropped below (median(autosomal windows) - 0.5)) for 10 consecutive 10KB windows; each differentiated region was extended along the chromosome as long as Log2(female/male coverage) did not rise above that threshold for 10 consecutive windows (regions shaded in gray in Fig. 1). The two largest differentiated regions were nearly adjacent on the distal end of chromosome 1, and the whole region encompassing them was classified as S0 (no genes were found in the small undifferentiated region between them, such that including it in the S0 did not affect downstream analyses). We used a similar approach to detect regions of increased male:female F_{ST}. In this case, only sparse information along the chromosome was obtained (as RNA-seq only provides SNPs for genic regions), and many 1kb bins were empty. We selected only informative bins, and inferred an F_{ST} rolling median for 30 bins at a time (the median coordinate for the bins was similarly used as the coordinate for the resulting window). High F_{ST} regions were called when 10 consecutive rolling windows were above the 95%-percentile of autosomal windows, and these regions were extended along the chromosome until 10 consecutive windows were below this threshold. This yielded three nearly-adjacent high F_{ST} sections (35.3-38.2MB, 38.4-67.3MB, 68.5-87.7MB), and the region encompassing them (35.3-87.7MB) was classified as S1. S1 was further divided into S1a, which showed drops in female:male coverage, and S1b, which did not. The coordinate of the beginning of the first differentiated region within S1 was used as the boundary between them.

Identification of candidate W-genes with k-mer analysis

We used a k-mer based subtraction approach (Elkrewi et al., 2021) based on the tools included in the BBMap package (Bushnell, 2014) on male and female genomic and RNA-seq data from *A. franciscana* and *A. sinica*. The pipeline was applied to each species separately. In *A. sinica,* two male and two female DNA libraries and two whole body RNA-seq replicates for

each sex were used (Tables S1 and S2). In *A. franciscana*, the analysis was performed using one male and one female DNA libraries and pools of two RNA-seq replicates of heads and gonads for each sex, along with one whole body male and female RNA-seq libraries (SRR14598203 and SRR14598204).

First, the shared 31-mers between the female DNA and RNA libraries were identified, and then any k-mers matching male libraries were removed. Female RNA-seq reads containing these female-specific k-mers [with minimum k-mer fraction of 0.6 (mkf=0.6)] were retrieved and assembled using Trinity (Grabherr *et al.* 2011), and the perl script from the Trinity package (get_longest_isoform_seq_per_trinity_gene.pl) was used to keep only the longest isoform. The male and female genomic libraries were mapped to the assembled transcripts using Bowtie2 (Langmead and Salzberg 2012 p. 2), and candidates with a sum of female perfect matches <=8 and a ratio of sum-of-females/sum-of-males <=2 were removed. The final set consisted of 402 transcripts in *A. franciscana* and 319 in *A. sinica*.

Mapping of W candidates to the *A. sinica* genome

The *A. sinica* and *A. franciscana* candidate W-derived transcripts were mapped to the *A. sinica* genome assembly with Parallel Blat (Wang and Kong 2019) with a translated query and database, and a minimum match score of 50. Only alignments with match scores above 100 were considered, and the mapping location with the strongest match score was considered for each transcript.

Transcriptome assemblies and expression analysis

The *A. sinica* male transcriptome was assembled from two replicates of male whole body RNA-seq data (Huylmans *et al.* 2021) using Trinity (Grabherr *et al.* 2011) in two different modes: denovo and genome-guided. The two assemblies were concatenated and then filtered using the tr2aacds.pl script from EvidentialGene (Gilbert 2019). The transcriptome was

annotated with the Pannzer annotation server (Törönen *et al.* 2018), and mapped to the *A. sinica* genome using the same procedure as described in section “Mapping of W candidates to the *A. sinica* genome”.

For the expression analysis, only the first isoform was kept for each gene, and only transcripts longer than 500bp were used in the analysis. The RNA-seq reads from the *A. sinica* heads, gonads, and thoraces of males and females (Huylmans *et al.* 2021) were mapped to the curated transcriptome and gene expression levels (in Transcripts per million, TPM) were obtained using Kallisto (version 0.46.2, Bray *et al.* 2016). Normalization was done using NormalyzerDE (Willforss *et al.* 2019).

Two different *A. franciscana* de novo transcriptome assemblies were made using Trinity. The first using pooled RNA-seq reads from male heads and testes (two replicates each, (Huylmans *et al.* 2019)), and the second using the published whole-body male RNA-seq library (SRR14598203, Jo *et al.* 2021b). The two assemblies were concatenated and then filtered using the tr2aacds.pl script from EvidentialGene, and mapped to the *A. sinica* genome using the same procedure as described in section “Mapping of W candidates to the *A. sinica* genome”.

Phylogenetic Trees

The W candidates of *A. sinica* and *A. franciscana* were mapped reciprocally to each other using pblat (v. 36x2 with default parameters, Wang and Kong 2019), and reciprocal best hits were considered shared candidates. The W candidates of the two species were further mapped to their respective uncollapsed male transcriptome assemblies (see previous section) with pblat (Wang and Kong 2019) with a translated query and database, and a minimum match score of 50. The transcripts with the highest mapping score to the W candidates were used as the putative Z homologs in their respective species.

The *Branchinecta lindahli* transcriptome (Schwentner *et al.* 2018) was downloaded from the Crustacean Phylogeny dataset on Harvard Dataverse (https://doi.org/10.7910/DVN/SM7DIU). *B.*

lindahli homologs of shared W-candidates were obtained by mapping the putative Z homologs of both species to the *B. lindahli* transcriptome using pblat (-minScore=50 -t=dnax -q=dnax) and retrieving the transcript with highest alignments score (using the customized script 2-besthitblat.pl). A transcript was considered a homolog if it mapped to at least one of the putative Z homologs of the two species, and when the two Z homologs mapped to different outgroup sequences, both outgroup sequences were retrieved and used to make two different alignments.

The shared W candidates of *A. sinica* and *A. franciscana*, their Z homologs, and the outgroup sequences were aligned using MAFFT (version v7.487, with the options "mafft --adjustdirection INPUT > OUTPUT", Katoh *et al.* 2002). The resulting alignments were fed to phylogeny.fr (Dereeper *et al.* 2008), where the alignment was curated using GBLOCKS (Talavera and Castresana 2007), and the phylogenetic tree was constructed using PhyML (Guindon *et al.* 2010). Trees were made only for sequences where the number of overlapping positions after gblocks was longer than 200bp. In the four instances where the curated alignment length with the outgroup was shorter than 200bp, we tried aligning the sequences without the outgroup. For the two cases where the resulting alignment length was longer than or equal 200bp, unrooted trees were made. The trees were then downloaded in the Newick format and visualized using itol.embl.de (Letunic and Bork 2019).

Heterozygosity analysis in asexual female and rare male

Illumina genomic sequencing was performed on a rare male and its asexual sister (both derived from an Aibi Lake *A. parthenogenetica* lineage), yielding around 115 million paired-end reads with a length of 125 nucleotides for each sample. The reads were quality- and adapter-trimmed with Trimmomatic-0.36 (Bolger *et al.* 2014), and mapped to the draft *Artemia sp. Kazakhstan* genome assembly using STAR v.2.6.0c (Dobin *et al.* 2013) with default settings.

We indexed the reference *A. sp. Kazakhstan* genome using SAMtools v.1.10 (Li *et al.* 2009), called the SNPs from BAM alignments with BCFtools v.1.10.2 (Li *et al.* 2009), then removed indels, filtered for quality of reads over 30 and coverage over 5 and below 100 with VCFtools v.0.1.15 (Danecek *et al.* 2011), and removed multiallelic sites with BCFtools.

We calculated the fraction of SNPs that lost heterozygosity in the rare male DNA in comparison with the asexual sister DNA. It was calculated and visualized in 500kb bins for each chromosome.

Crossing design to identify the asexuality locus

We designed a backcross in order to investigate the loci controlling asexuality. An asexual female from Aibi Lake produced a rare male. We crossed this male with an inbred female from the closest related sexual species, *A. sp. Kazakhstan*. This produced asexual females and males in the F1 generation. We then backcrossed 12 males from the F1 to sexual females from from the same inbred line of *A. sp. Kazakhstan*. Of these, 6 crosses produced offspring, yielding a total of 84 males, 5 asexual females, and 96 putatively sexual females (those that did not reproduce asexually for 133 days after the crosses were set up). The 5 asexual females and 10 control females were used individually for DNA extractions with the Qiagen DNeasy Blood & Tissue kit. The control females came from the same crosses (i.e., had the same F2 father and *A. sp. Kazakhstan* mothers) as the asexual females, but were otherwise selected randomly. Illumina short-read sequencing was then performed as described in section “DNA short and long read sequencing”.

Analysis of backcross between the Aibi Lake rare male and *A. sp. Kazakhstan* females

We sequenced 5 asexual females and 10 putatively sexual females from the F2 generation. This resulted in an average of 101 million reads per asexual female and 50 million reads per putatively sexual female. We first used SEQTK v1.2 (https://github.com/lh3/seqtk) to randomly

select a subset of reads from each asexual sample to match the number of reads of the smallest sample (to avoid biasing allele estimates towards high-coverage individuals). We removed adaptors and trimmed reads using Trimmomatic v0.39 (Bolger *et al.* 2014). We then aligned the resulting paired-end reads to the genome using Bowtie2 v2.4.4 (Langmead and Salzberg 2012). SAM files were converted to BAM files and sorted in Samtools v.1.13 (Li *et al.* 2009).

For our pooled analyses, we merged BAM files into a pooled asexual BAM file and a pooled putatively-sexual BAM, and created a mpileup file in Samtools v.1.13. We then used Popoolation2 (Kofler *et al.* 2011) to call F_{ST} for both individual SNPs and in 1kb windows. We used F_{ST} computed for 1kb windows to visualize F_{ST} across the genome in a Manhattan plot in the R package qqman (Turner 2018). We computed rolling medians in sliding windows of 101 consecutive SNPs on each linkage group using the rollmedian function from the package zoo (Zeileis and Grothendieck 2005) in R v.4.0.3. To identify regions of elevated F_{ST} on individual chromosomes, we computed 95% confidence intervals by sampling rolling medians of 101 consecutive SNPs across the genome 1000 times.

For our individual-based analyses, we similarly used SEQTK v1.2 to randomly select a subset of reads from each asexual sample to match the highest coverage found in an F2 control female (to avoid biases caused by the much larger number of reads obtained for the F2 asexuals than for the controls). We then mapped reads from all F2 individuals to the *A. sp. Kazakhstan* genome using BWA mem v0.7.17 (Li and Durbin 2009) with default parameters. DNA reads from the rare male and its *A. parthenogenetica* sister, and from two *A. sp. Kazakhstan* individuals, were also subsetted and mapped. The resulting BAM alignments were sorted with samtools v1.14 (Li *et al.* 2009), and used to call SNPs with the mpileup function of BCFtools v1.14 (Li 2011). The VCF file was filtered with VCFtools v0.1.17 (Danecek *et al.* 2011) for minimum and maximum depth (4 and 50), minimum quality score (30) and minimum minor allele frequency (0.1). Only SNPs for which the two *A. sp. Kazakhstan* had a genotype of 0/0,

and the two *A. parthenogenetica* individuals 1/1, were kept for further analyses. We computed F_{ST} between the F2 asexual and control females using the function --weir-fst-pop in VCFtools for 10kb windows. We then inferred ancestry of each genomic scaffold in every sample (i.e., whether they were homozygous for the *A. sp. Kazakhstan* haplotype, or carried a copy of the *A. parthenogenetica* haplotype as well) using the customized script Chromopaint.pl (available on our git page). The *A. sp. Kazakhstan* genomic scaffolds were assigned to a location on the *A. sinica* genome as before. Scaffolds with more than 10 informative SNPs, and >80% 0/1 or 1/1 SNPs were considered to be heterozygous for the *A. sp. Kazakhstan* and *A. parthenogenetica* haplotypes, whereas scaffolds with >80% 0/0 were considered to have only *A. sp. Kazakhstan* ancestry (only 5 to 9% of scaffolds fell in between and could not be classified in each individual).

Results

1. The ZW pair is shared by American and Eurasian *Artemia*

Two genome assemblies and a high-density linkage map are currently available for the American *A. franciscana* (Jo *et al.* 2021a; Han *et al.* 2021; De Vos *et al.* 2021), but resources for the Eurasian clade are more limited, with only an *A. sp. Kazakhstan* draft genome assembly recently described in Boyer et al. (2022). The median dS (the number of synonymous substitutions per synonymous site) between the two clades is ~0.2. We assembled a male genome of *A. sinica* using PacBio long reads (~30x) and Hi-C Illumina reads (1.5*e12 reads), yielding 1213 scaffolds with an N50 of 67.19 Mb (Fig. S2, Table S3) and a total length of 1.7Gb; 85% of the sequences get assigned to one of the 21 largest scaffolds (which corresponds to the expected number of chromosomes, Sainz-Escudero *et al.* 2021). The strong diagonal in the heatmap of the Hi-C contact matrix (Fig. S3) supports the high quality of our assembly, as does our BUSCO score of 91.8%. This chromosome-level assembly represents an improvement over existing *Artemia* genomes, which have N50 values of 27 to 112Kb, and BUSCO scores of 68.3% to 86.9% (Jo *et al.* 2021a; De Vos *et al.* 2021; Boyer *et al.* 2022; Fig. S4).

Our earlier analysis of female and male genomic coverage in *A. franciscana* had uncovered a small region of reduced female coverage, consistent with full differentiation of the Z and W chromosomes (Huylmans *et al.* 2019). To investigate whether ZW differentiation was also present in *A. sinica*, we first estimated male and female coverage along each chromosome. Consistent with *A. franciscana*, only a small genomic region on chromosome 1 had decreased female/male coverage (Fig. 1A, Fig. S5 for all chromosomes), showing that chromosome 1 is the Z chromosome. To check for homology with the *A. franciscana* differentiated region, we mapped the scaffolds from the *A. franciscana* genome of (Jo *et al.* 2021a) to the new *A. sinica* assembly based on their shared gene content, and plotted the coverage values that we had previously estimated (Huylmans *et al.* 2019) based on the *A. sinica* coordinates. Fig. 1A shows that the two differentiated regions largely overlap, supporting the ancestry of the pair of sex chromosomes; we name this shared region stratum 0 (S0). In the *A. franciscana* linkage map (Han *et al.* 2021), LG6 was identified as the sex chromosome. To further verify the homology between the ZW pairs of the two species, we mapped the genetic markers used by Han et al. (2021) to our *A. sinica* assembly. As expected, the vast majority of LG6 markers for which we could infer a location mapped to our chromosome 1 (Fig. S6). We also produced an assembly based on *A. sinica* female long PacBio reads, which contains a substantial amount of scaffolds with excessive female coverage, consistent with W-linkage (Fig. S7).

2. Convergent loss of ZW recombination

To identify parts of the sex chromosomes that no longer recombine, but are still similar enough that W-derived reads still map to the Z, we used previously published RNA-seq data for *A. sinica* (Huylmans *et al.* 2021), obtained from 10 males and 10 females, to estimate F_{ST}, a measure of genetic differentiation, between the two sexes. Genetic variants found exclusively on the W increase the level of female-male differentiation, and young non-recombining regions can be detected through their high male:female F_{ST} (Palmer *et al.* 2019; Vicoso 2019;

Gammerdinger *et al.* 2020). Such an increase in male:female F_{ST} is not expected for the highly differentiated S0, since W-derived reads do not map to this part of the Z-chromosome. Fig. 1B shows that a large region (~52 Mb) has F_{ST} values systematically above the 95th-percentile of autosomes, consistent with recent loss of recombination in *A. sinica*. We call this region Stratum 1 (S1), but further divide it into S1a, which shows localized drops in female:male coverage (gray shaded regions in Fig. 1A), and S1b, for which no coverage differences are observed (Fig. 1A), and which may still undergo some recombination. The distal end of S1a has reduced female:male coverage in *A. franciscana*, and an F_{ST} analysis in this species yielded increased male:female FST from ~60 to 85MB (see Fig. S8), showing that at least part of this region has also stopped recombining in the American lineage.

Given the substantial distance between the Eurasian and American lineages, we hypothesized that the loss of recombination in S1 had occurred independently in the two clades. To test this, we used a k-mer-based pipeline combining male and female DNA and RNA short reads (Elkrewi *et al.* 2021) to identify putative W-derived transcripts. This yielded 402 transcripts in *A. franciscana* and 319 in *A. sinica*. Of those that mapped to the genome, 180 out of 306 (59%) *A. sinica* transcripts and 168 out of 355 (47%) *A. franciscana* transcripts mapped to chromosome 1 (Z) of *A. sinica*, a higher proportion than the overall 7% of genes that map to this chromosome, confirming the validity of the approach (since we expect many W-linked genes to have a close homolog on the Z). Few of these candidate W genes mapped to the putative ancestral sex-linked region (16 W-linked genes in *A. sinica*, compared to 84 Z-linked genes, and 7 versus 91 in *A. franciscana*, Table S4), consistent with substantial degeneration of this part of the W-chromosome. To find genes present on the W-chromosomes of both species, we selected reciprocal best hits between the two sets of W candidates. All 15 candidates that were found in both species mapped to the putative S1a region. We made phylogenetic trees using each pair of homologous W-genes and their Z-linked homologs (obtained from a male-only transcriptome assembly, and all mapping to the S1a region), to infer whether these genes were

W-linked before the split of the two clades. The closest homolog in the transcriptome of the distantly related fairy shrimp *Branchinecta lindahli* (Schwentner *et al.* 2018) was used as an outgroup sequence, when one could be detected. Fig. 1C shows the resulting phylogenetic trees for two of the shared W-linked genes and their Z-homologs, while phylogenies for all candidates are provided in Fig. S9. In every case, ZW homologs clustered by species rather than by chromosome, confirming that loss of recombination occurred independently and convergently for this region in the American and Eurasian lineages.

3. Dosage compensation of the Z-specific region

Many female-heterogametic species lack a chromosome-wide mechanism of dosage compensation, and investigating the few cases that have it may shed light on the difference between ZW and XY systems. Earlier work suggested that the Z-specific region of *A. franciscana* was compensated (Huylmans *et al.* 2019), but misidentification of genes in the sex-linked region (as the genome was fragmented) could have hidden differences between chromosomes. We repeated this analysis using RNA-seq data from thorax, head, and gonad of *A. sinica* (Huylmans et al. 2021). We first assembled a male transcriptome from all pooled male reads available for this species (to avoid hybrid assemblies of Z and W homologs, see Fig. S10 for a BUSCO assessment), mapped it to the male genome assembly, and estimated expression for each sample (in transcripts per million, TPM). In somatic tissues, the female:male ratio is similar for the autosomal genes and S0 genes ($p = 0.2$ and $p = 0.6$ in heads and thoraces, Bonferroni-corrected Wilcoxon tests, Fig. 2B and 2C), confirming that dosage compensation is active in this clade. A significant shift towards male-biased expression can be observed for the S0 in gonads ($p = 0.0007$, Bonferroni-corrected Wilcoxon test, Fig. 2D). A table with nominal p-values for each comparison is provided in Table S5.

513 **4. The sex chromosomes of asexual females and the genetic origin of rare males**

514 In order to characterize the ZW pair of asexual females, we first obtained a draft genome
515 assembly of the closely related sexual species *A. sp. Kazakhstan* from illumina short reads
516 (Table S6), and estimated genomic coverage using two female and two male samples of this
517 species. The genomic scaffolds were mapped to the *A.sinica* genome based on their gene
518 content, and median coverages of male and female *A. sp. Kazakhstan* individuals were plotted
519 along the *A. sinica* Z chromosome using a sliding window of 10 scaffolds (green and yellow
520 lines in Fig. 3A). As expected, an approximately two-fold drop in female coverage was observed
521 in a similar region to that found in *A. sinica* (marked by gray shading), whereas the male
522 harbored high genomic coverage throughout the chromosome, consistent with the presence of
523 the same pair of sex chromosomes in this lineage (a similar pattern was observed in *A.*
524 *urmiana*, Fig. S11). We used the *A. sp. Kazakhstan* draft genome to map genomic reads
525 derived from three closely related asexual females (one from the Lake Urmiana-derived
526 population, and two from a population derived from Aibi Lake cysts). In every case, the patterns
527 of coverage were very similar to those of the *A. sp. Kazakhstan* sexual female, confirming that
528 asexual females carry the same pair of ZW chromosomes.

529 Diploid *A. parthenogenetica* likely reproduce through central fusion automixis, a modified
530 form of meiosis that preserves heterozygosity in the genome except at distal ends of
531 chromosomes when recombination has occurred (Nougué *et al.* 2015). Boyer *et al.* (2022)
532 recently showed that *Artemia* rare males can be produced by ZW recombination events at
533 variable locations near the sex-determining locus. We obtained a rare male from an *A.*
534 *parthenogenetica* line from Aibi Lake (which we use in the next section to explore the
535 transmission of asexuality). To test whether it arose through ZW recombination or other
536 chromosomal changes, we first compared patterns of genomic coverage to those of females. No
537 reduced coverage was observed along the Z-chromosome, arguing against the loss of a sex
538 chromosome. We further called Single Nucleotide Polymorphisms (SNPs) in the rare male and

in its sister (marked as A. par. Aibi lake 2 in Fig 3A), and estimated the proportion of heterozygous SNPs present in the asexual female that were lost in the rare male. Loss of heterozygosity was detected throughout the distal half of the Z-chromosome (Fig. 3B and Fig. S12), confirming that a large part of the W was replaced by its Z homologous region. A substantial loss of heterozygosity was also found at the beginning of chr 13, and smaller regions of decreased heterozygosity may be present at the ends of several chromosomes (Fig. S12). Taken together, these results support central fusion automixis as the mode of reproduction of *A. parthenogenetica*, and rare ZW recombination as the source of the Aibi Lake rare male (Nougué *et al.* 2015; Boyer *et al.* 2022).

5. The Z chromosome likely contributes to the transmission of asexuality

In order to find possible loci responsible for the spread of asexuality in brine shrimp, we crossed the rare male described in the previous section and a sexual female from *A. sp. Kazakhstan* (Fig. S13). This produced 22 asexual females and 24 males in the F1; one additional female died without producing offspring asexually. The presence of asexual females in the F1 shows that the locus controlling asexuality in this lineage works in a dominant manner, unlike what was first observed in (Maccari *et al.* 2014), but consistent with the recent experiments of Boyer *et al.* (2021). The fact that almost all females produced offspring without mating further suggests that the locus was likely present on both copies of the genome of the original rare male. We then backcrossed 12 males from the F1, which should only carry one copy of the locus/loci controlling asexuality, with females from an *A. sp. Kazakhstan* inbred line (of these only 6 yielded progeny). The resulting F2 generation consisted of 84 (~45%) males, 5 (~3%) asexual females, and 96 (~52%) females that did not produce asexually 133 days after the crosses were set up (44 individuals died before sexing was possible and are not included in the counts; see counts for individual crosses in Table S7). We presume that most of these are

564 sexual females for our analyses, but some could have reproduced asexually had the experiment
565 been continued longer.

566 We produced whole-genome resequencing data for the 5 F2 asexual females and, as a
567 control, 10 F2 putatively sexual females. These were first pooled into an asexual pool and a
568 putatively sexual pool, and we used Popoolation2 to compute F_{ST} between these two pools of
569 females. While a few small peaks of F_{ST} are found on the autosomes (Fig 4a), the strongest
570 signal comes from the distal end of the Z chromosome (Fig 4b). We further predicted that loci
571 underlying asexuality should have been inherited from the original rare male by all the F2
572 asexual females, but not by (all) control females. To test this, we mapped all DNA samples
573 individually to the *A. sp. Kazakhstan* genome. We also mapped the original rare male and its *A.*
574 *parthenogenetica* sister, and two *A. sp. Kazakhstan* individuals, in order to select SNPs that
575 were alternatively fixed between the two lineages. We used these informative SNPs to
576 reestimate F_{ST} between F2 asexual and control females, and to infer which genomic regions
577 were inherited from the rare male by each of the F2 individuals. Fig. S14 shows that we recover
578 a region of high F_{ST} on the Z chromosome, and that all asexuals carry genetic material from the
579 rare male in this region, as expected if it controls asexuality. In total, only 17 scaffolds with an
580 assigned location on the *A. sinica* genome show ancestry patterns consistent with an asexuality
581 locus (i.e., they show evidence of *A. parthenogenetica* ancestry in all asexual females, but not in
582 all control females). Eleven are on the Z chromosome (versus 1 expected, p=1.3e-20 with a
583 Chi-square test), and correspond to the region of high F_{ST}, providing further support for a role of
584 the Z chromosome in the transmission of asexuality. None of the other minor peaks of F_{ST} are in
585 regions with ancestry patterns consistent with asexuality loci (Fig. S14), although chromosome
586 16 contains 3 such loci (versus 0.9 expected, $p<0.01$ with a chi-square test). The annotation of
587 genes located in the Z-linked candidate locus did not yield any obvious candidates (the
588 annotation for all transcripts is provided as a Supplementary Dataset).
589

Discussion

The potential of Artemia brine shrimp as models for ZW chromosome evolution and comparative genomics in general was until recently hampered by a lack of genomic resources. The publication of two genomes for the American *A. franciscana* has already shed new light on how these charismatic organisms survive in their extreme environments (Jo *et al.* 2021a; De Vos *et al.* 2021), but no information on sex linkage was provided, and the lack of a close outgroup sequence (other than the distant Daphnia) made comparative analyses difficult. A draft genome was recently described for *A. sp. Kazakhstan* (Boyer *et al.* 2022), but there was limited power to assign scaffolds to the sex chromosomes or autosomes.

Here, we obtain the first chromosome-level assembly in the clade for the Eurasian brine shrimp *A. sinica*, and characterize in detail the differentiated and undifferentiated regions of the ZW pair. By combining these results with those of a preliminary analysis in *A. franciscana* (Huylmans *et al.* 2019), we confirmed the putative evolutionary model for the ZW pair, with an ancient well-differentiated region that stopped recombining in the ancestor of the two lineages, and more recent “strata” arising in each lineage independently. The independent loss of recombination in American and Eurasian species provides a unique opportunity to investigate convergent changes that occur in early sex-chromosome evolution. In agreement with previous findings in *A. franciscana*, *A. sinica* males and females have similar somatic expression patterns of Z-linked genes in the differentiated region which strongly supports the presence of a mechanism of dosage compensation in this group. A significant male-bias in expression was found for S0 genes in the gonads. Such differences in the gonad have been found even in animals with well-characterized chromosome-wide mechanisms of dosage compensation, such as Drosophila (Meiklejohn et al. 2011) and silkworm (Huylmans *et al.* 2017). While compensation mechanisms may be absent or less active in the gonad (Meiklejohn *et al.* 2011) , differences could also result from the unusual regulation of the sex chromosomes in the germline (Argyridou and Parsch 2018), where they are often inactivated or downregulated

(Vibranovski *et al.* 2009). Currently, no tractable lab model exists for the early evolution of ZW chromosomes, and Z-chromosome dosage compensation is only understood in detail for the silkworm (Walters and Hardcastle 2011; Kiuchi *et al.* 2014; Katsuma *et al.* 2019; Rosin *et al.* 2022), making this an outstanding new model clade for investigating these topics.

Finally, we obtained several putative W-genes in both species using a k-mer based analysis. Few of them mapped to the ancestral part of the W chromosome: only ~20% of the Z-linked genes in this region have a W-homolog, suggesting that much of the ancestral gene content has been lost. All of the genes for which a W-homolog could be found in both *A. sinica* and *A. franciscana* mapped to younger strata of the ZW pair, and appear to have become W-linked independently in the two lineages. If the ancestral sex-determination mechanism is still shared by the two species, this may suggest that the primary signal for sex determination is a dosage-dependent gene on the Z rather than a dominant female-determining gene on the W. However, it is also possible that the sex-determining gene is only expressed early in development, and was missed by our analysis of adult tissues. Future studies of sex-specific expression throughout the life cycle and complete assemblies of the W chromosome of the two species will be necessary to shed light on sex determination in this group.

The proximity of *A. sinica* to the *A. sp. Kazakhstan* group, which contains both sexual and asexual populations, also allowed to characterize sex-linked sequences in this group. First, we found that the sex chromosome pair is shared by all populations. We further confirmed that rare males in this group can be produced through the replacement of the W-specific region with its Z-counterpart, showing that the same mechanism is used for rare male production in *A. parthenogenetica* isolates from widely differing geographic origins (China in this study, Iran and France in Boyer et al., 2022). Finally, our backcrossing experiment points to a role of the sex chromosome pair in the spread of asexuality through rare males.

It should be noted that this experiment has several drawbacks. First, it is difficult to phenotype females as sexual or asexual, as the timing at which asexuals produce their first

642 brood can vary (although they typically do so within 30 days of hatching, Amat *et al.* 2007).
643 Furthermore, hybrid incompatibilities may stop females from producing viable offspring even if
644 they carry the alleles encoding asexuality. The fact that only ~5% of females were asexual in
645 the F2 suggests that either the trait is polygenic, and/or that we are mistakenly classifying
646 asexuals as putative sexuals. Finally, we only obtained a small number of backcrossed asexual
647 females, which limits the power to infer causal loci.
648 Despite these drawbacks, the Z chromosome showing the strongest signal of
649 differentiation between asexual and control females is intriguing, and in line with results in the
650 pea aphid, which carries the asexuality locus on the X chromosome. In species where
651 asexuality is triggered by an endoparasite such as Wolbachia, the acquisition of asexuality is
652 thought to be driven by the transmission advantage gained by the female-transmitted parasite
653 (since asexual reproduction leads to an all-female progeny). It is possible that an asexuality
654 gene found on a Z chromosome similarly benefits from a transmission advantage. If rare males
655 always arise through the replacement of the W-specific region with its Z homolog region, a Z-
656 linked asexuality locus will be homozygous and therefore transmitted to all daughters in the F1
657 (and to all sons). More detailed studies of transmission of asexuality in this group and others
658 with ZW and XY sex chromosomes will in the future shed light on the relationship between sex
659 determination and the rise and spread of asexual reproduction under various sex-determining
660 mechanisms.
661
662 **Data availability statement**
663 All genomic reads generated for this study are available at the NCBI short reads archive
664 under Bioproject number PRJNA848277. The pipelines used to analyze the data are at
665 https://git.ist.ac.at/bvicoso/zsexasex2021, and important processed data files such as the new
666 *A. sinica* genome assembly are provided at https://doi.org/10.15479/AT:ISTA:11653.
667

668 **Acknowledgements**

669 We thank the Vicoso group for comments on the manuscript, and the ISTA Scientific computing
670 team and the Vienna Biocenter Sequencing facility for technical support.

671

672 **Funding and Competing Interests**

673 This work was supported by the European Research Council under the European Union's
674 Horizon 2020 research and innovation program (grant agreement no. 715257), and by the
675 Austrian Science Foundation (FWF SFB F88-10).

676

677

678

679 **Reference**

680 Abatzopoulos T. J., 2018 The repeated emergence of asexuality, the hidden genomes and the
681 role of parthenogenetic rare males in the brine shrimp Artemia. J. Biol. Res.-Thessalon.
682 25: 7. https://doi.org/10.1186/s40709-018-0078-2

683 Accioly I. V., I. M. C. da Cunha, J. C. M. Tavares, and W. F. Molina, 2015 CHROMOSOME
684 BANDING IN CRUSTACEA. I. KARYOTYPE, Ag-NORs, C BANDING AND
685 TREATMENT WITH EcoRI, PstI and KpnI RESTRICTION ENDONUCLEASES IN
686 Artemia franciscana. Biota Amaz. Biote Amaz. Biota Amazon. Amaz. Biota.

687 Amat F., F. Hontoria, J. C. Navarro, N. Vieira, and G. Mura, 2007 Biodiversity loss in the genus
688 Artemia in the Western Mediterranean Region. Limnética 26: 387–404.

689 Argyridou E., and J. Parsch, 2018 Regulation of the X Chromosome in the Germline and Soma
690 of Drosophila melanogaster Males. Genes 9: 242. https://doi.org/10.3390/genes9050242

691 Arima Genomics, 2021 *mapping_pipeline*. Arima Genomics, Inc.
692 https://github.com/ArimaGenomics/mapping_pipeline

693 Aumer D., M. H. Allsopp, H. M. G. Lattorff, R. F. A. Moritz, and A. Jarosch-Perlow, 2017
694 Thelytoky in Cape honeybees (Apis mellifera capensis) is controlled by a single
695 recessive locus**.** Apidologie volume 48, pages 401–410.

696 Bachtrog D., 2013 Y-chromosome evolution: emerging insights into processes of Y-
697 chromosome degeneration. Nat. Rev. Genet. 14: 113–124.
698 https://doi.org/10.1038/nrg3366

699 Bachtrog D., J. E. Mank, C. L. Peichel, M. Kirkpatrick, S. P. Otto, *et al.*, 2014 Sex
700 Determination: Why So Many Ways of Doing It? PLOS Biol. 12: e1001899.
701 https://doi.org/10.1371/journal.pbio.1001899

702 Baxevanis A. D., I. Kappas, and T. J. Abatzopoulos, 2006 Molecular phylogenetics and
703 asexuality in the brine shrimp Artemia. Mol. Phylogenet. Evol. 40: 724–738.
704 https://doi.org/10.1016/j.ympev.2006.04.010

Beukeboom L. W., and N. Perrin, 2014 *The Evolution of Sex Determination*. Oxford University Press, Oxford.

Bolger A. M., M. Lohse, and B. Usadel, 2014 Trimmomatic: a flexible trimmer for Illumina sequence data. Bioinformatics 30: 2114–2120. https://doi.org/10.1093/bioinformatics/btu170

Bowen S. T., 1963 The Genetics of Artemia salina. III. Effects of X-Irradiation and of Freezing upon Cysts. Biol. Bull. 125: 431–440. https://doi.org/10.2307/1539357

Boyer L., R. Jabbour-Zahab, M. Mosna, C. R. Haag, and T. Lenormand, 2021 Not so clonal asexuals: Unraveling the secret sex life of Artemia parthenogenetica. Evol. Lett. 5: 164–174. https://doi.org/10.1002/evl3.216

Boyer L., R. Jabbour-Zahab, P. Joncour, S. Glémin, C. R. Haag, *et al.*, 2022 Asexual male production by ZW recombination in Artemia parthenogenetica. bioRxiv 2022.04.01.486774; doi: https://doi.org/10.1101/2022.04.01.486774

Bray N. L., H. Pimentel, P. Melsted, and L. Pachter, 2016 Near-optimal probabilistic RNA-seq quantification. Nat. Biotechnol. 34: 525–527. https://doi.org/10.1038/nbt.3519

Bushnell B., 2014 BBMap: A Fast, Accurate, Splice-Aware Aligner**.** No. LBNL-7065E. Ernest Orlando Lawrence Berkeley National Laboratory, Berkeley, CA.

Chakraborty M., J. G. Baldwin-Brown, A. D. Long, and J. J. Emerson, 2016 Contiguous and accurate de novo assembly of metazoan genomes with modest long read coverage. Nucleic Acids Res. 44: e147. https://doi.org/10.1093/nar/gkw654

Charlesworth B., 1978 Model for evolution of Y chromosomes and dosage compensation. Proc. Natl. Acad. Sci. 75: 5618–5622. https://doi.org/10.1073/pnas.75.11.5618

Charlesworth D., B. Charlesworth, and G. Marais, 2005 Steps in the evolution of heteromorphic sex chromosomes. Heredity 95: 118–128. https://doi.org/10.1038/sj.hdy.6800697

Charlesworth D., 2019 Young sex chromosomes in plants and animals. New Phytol. 224: 1095–1107. https://doi.org/10.1111/nph.16002

731 Danecek P., A. Auton, G. Abecasis, C. A. Albers, E. Banks, *et al.*, 2011 The variant call format
732 and VCFtools. Bioinformatics 27: 2156–2158.
733 https://doi.org/10.1093/bioinformatics/btr330
734 De Vos S., P. Bossier, G. Van Stappen, I. Vercauteren, P. Sorgeloos, *et al.*, 2013 A first AFLP-
735 based genetic linkage map for brine shrimp Artemia franciscana and its application in
736 mapping the sex locus. PloS One 8: e57585.
737 https://doi.org/10.1371/journal.pone.0057585
738 De Vos S., S. Rombauts, L. Coussement, W. Dermauw, M. Vuylsteke, *et al.*, 2021 The genome
739 of the extremophile Artemia provides insight into strategies to cope with extreme
740 environments. BMC Genomics 22: 635. https://doi.org/10.1186/s12864-021-07937-z
741 Dereeper A., V. Guignon, G. Blanc, S. Audic, S. Buffet, *et al.*, 2008 Phylogeny.fr: robust
742 phylogenetic analysis for the non-specialist. Nucleic Acids Res. 36: W465–W469.
743 https://doi.org/10.1093/nar/gkn180
744 Disteche C. M., 2016 Dosage compensation of the sex chromosomes and autosomes. Semin.
745 Cell Dev. Biol. 56: 9–18. https://doi.org/10.1016/j.semcdb.2016.04.013
746 Dobin A., C. A. Davis, F. Schlesinger, J. Drenkow, C. Zaleski, *et al.*, 2013 STAR: ultrafast
747 universal RNA-seq aligner. Bioinformatics 29: 15–21.
748 https://doi.org/10.1093/bioinformatics/bts635
749 Eads B. D., D. Tsuchiya, J. Andrews, M. Lynch, and M. E. Zolan, 2012 The spread of a
750 transposon insertion in Rec8 is associated with obligate asexuality in Daphnia. Proc.
751 Natl. Acad. Sci. 109: 858–863. https://doi.org/10.1073/pnas.1119667109
752 Elkrewi M., M. A. Moldovan, M. A. L. Picard, and B. Vicoso, 2021 Schistosome W-Linked Genes
753 Inform Temporal Dynamics of Sex Chromosome Evolution and Suggest Candidate for
754 Sex Determination. Mol. Biol. Evol. 38: 5345–5358.
755 https://doi.org/10.1093/molbev/msab178
756 Ellegren H., 2011 Sex-chromosome evolution: recent progress and the influence of male and

757 female heterogamety. Nat. Rev. Genet. 12: 157–166. https://doi.org/10.1038/nrg2948
758 Gammerdinger W. J., M. A. Toups, and B. Vicoso, 2020 Disagreement in F ST estimators: A
759 case study from sex chromosomes. Mol. Ecol. Resour. 20: 1517–1525.
760 https://doi.org/10.1111/1755-0998.13210
761 Gilbert D. G., 2019 Longest protein, longest transcript or most expression, for accurate gene
762 reconstruction of transcriptomes? bioRxiv 829184; doi: https://doi.org/10.1101/829184.
763 Grabherr M. G., B. J. Haas, M. Yassour, J. Z. Levin, D. A. Thompson, *et al.*, 2011 Trinity:
764 reconstructing a full-length transcriptome without a genome from RNA-Seq data. Nat.
765 Biotechnol. 29: 644–652. https://doi.org/10.1038/nbt.1883
766 Guan D., S. A. McCarthy, J. Wood, K. Howe, Y. Wang, *et al.*, 2020 Identifying and removing
767 haplotypic duplication in primary genome assemblies. Bioinformatics 36: 2896–2898.
768 https://doi.org/10.1093/bioinformatics/btaa025
769 Guindon S., J.-F. Dufayard, V. Lefort, M. Anisimova, W. Hordijk, *et al.*, 2010 New algorithms
770 and methods to estimate maximum-likelihood phylogenies: assessing the performance
771 of PhyML 3.0. Syst. Biol. 59: 307–321. https://doi.org/10.1093/sysbio/syq010
772 Haag C. R., L. Theodosiou, R. Zahab, and T. Lenormand, 2017 Low recombination rates in
773 sexual species and sex–asex transitions. Philos. Trans. R. Soc. B Biol. Sci. 372:
774 20160461. https://doi.org/10.1098/rstb.2016.0461
775 Han X., Y. Ren, X. Ouyang, B. Zhang, and L. Sui, 2021 Construction of a high-density genetic
776 linkage map and QTL mapping for sex and growth traits in Artemia franciscana.
777 Aquaculture 540: 736692. https://doi.org/10.1016/j.aquaculture.2021.736692
778 Handley L.-J. L., H. Ceplitis, and H. Ellegren, 2004 Evolutionary strata on the chicken Z
779 chromosome: implications for sex chromosome evolution. Genetics 167: 367–376.
780 Huylmans A. K., A. Macon, and B. Vicoso, 2017 Global Dosage Compensation Is Ubiquitous in
781 Lepidoptera, but Counteracted by the Masculinization of the Z Chromosome. Mol. Biol.
782 Evol. 34: 2637–2649. https://doi.org/10.1093/molbev/msx190

783 Huylmans A. K., M. A. Toups, A. Macon, W. J. Gammerdinger, and B. Vicoso, 2019 Sex-Biased
784 Gene Expression and Dosage Compensation on the Artemia franciscana Z-
785 Chromosome. Genome Biol. Evol. 11: 1033–1044. https://doi.org/10.1093/gbe/evz053
786 Huylmans A. K., A. Macon, F. Hontoria, and B. Vicoso, 2021 Transitions to asexuality and
787 evolution of gene expression in Artemia brine shrimp. Proc. Biol. Sci. 288: 20211720.
788 https://doi.org/10.1098/rspb.2021.1720
789 Jaquiéry J., S. Stoeckel, C. Larose, P. Nouhaud, C. Rispe, *et al.*, 2014 Genetic Control of
790 Contagious Asexuality in the Pea Aphid. PLOS Genet. 10: e1004838.
791 https://doi.org/10.1371/journal.pgen.1004838
792 Jo E., S. J. Lee, E. Choi, J. Kim, S. G. Lee, *et al.*, 2021a Whole genome survey and
793 microsatellite motif identification of Artemia franciscana. Biosci. Rep. 41: BSR20203868.
794 https://doi.org/10.1042/BSR20203868
795 Jo E., S.-J. Lee, E. Choi, J. Kim, J.-H. Lee, *et al.*, 2021b Sex-Biased Gene Expression and
796 Isoform Profile of Brine Shrimp Artemia franciscana by Transcriptome Analysis. Anim.
797 Open Access J. MDPI 11: 2630. https://doi.org/10.3390/ani11092630
798 Kampfraath A. A., T. P. Dudink, K. Kraaijeveld, J. Ellers, and Z. V. Zizzari, 2020 Male Sexual
799 Trait Decay in Two Asexual Springtail Populations Follows Neutral Mutation
800 Accumulation Theory. Evol. Biol. 47: 285–292. https://doi.org/10.1007/s11692-020-
801 09511-z
802 Katoh K., K. Misawa, K. Kuma, and T. Miyata, 2002 MAFFT: a novel method for rapid multiple
803 sequence alignment based on fast Fourier transform. Nucleic Acids Res. 30: 3059–
804 3066. https://doi.org/10.1093/nar/gkf436
805 Katsuma S., K. Shoji, Y. Sugano, Y. Suzuki, and T. Kiuchi, 2019 Masc-induced dosage
806 compensation in silkworm cultured cells. FEBS Open Bio 9: 1573–1579.
807 https://doi.org/10.1002/2211-5463.12698
808 Kent W. J., 2002 BLAT--the BLAST-like alignment tool. Genome Res. 12: 656–664.

https://doi.org/10.1101/gr.229202

Kiuchi T., H. Koga, M. Kawamoto, K. Shoji, H. Sakai, *et al.*, 2014 A single female-specific piRNA is the primary determiner of sex in the silkworm. Nature 509: 633–636. https://doi.org/10.1038/nature13315

Kofler R., R. V. Pandey, and C. Schlötterer, 2011 PoPoolation2: identifying differentiation between populations using sequencing of pooled DNA samples (Pool-Seq). Bioinformatics 27: 3435–3436. https://doi.org/10.1093/bioinformatics/btr589

Kolmogorov M., J. Yuan, Y. Lin, and P. A. Pevzner, 2019 Assembly of long, error-prone reads using repeat graphs. Nat. Biotechnol. 37: 540–546. https://doi.org/10.1038/s41587-019-0072-8

Lahn B. T., and D. C. Page, 1999 Four evolutionary strata on the human X chromosome. Science 286: 964–967. https://doi.org/10.1126/science.286.5441.964

Langmead B., and S. L. Salzberg, 2012 Fast gapped-read alignment with Bowtie 2. Nat. Methods 9: 357–359. https://doi.org/10.1038/nmeth.1923

Lenormand T., F. Fyon, E. Sun, and D. Roze, 2020 Sex Chromosome Degeneration by Regulatory Evolution. Curr. Biol. 30: 3001-3006.e5. https://doi.org/10.1016/j.cub.2020.05.052

Lenormand T., and D. Roze, 2022 Y recombination arrest and degeneration in the absence of sexual dimorphism. Science 375: 663–666. https://doi.org/10.1126/science.abj1813

Letunic I., and P. Bork, 2019 Interactive Tree Of Life (iTOL) v4: recent updates and new developments. Nucleic Acids Res. 47: W256–W259. https://doi.org/10.1093/nar/gkz239

Li H., and R. Durbin, 2009 Fast and accurate short read alignment with Burrows-Wheeler transform. Bioinforma. Oxf. Engl. 25: 1754–1760. https://doi.org/10.1093/bioinformatics/btp324

Li H., B. Handsaker, A. Wysoker, T. Fennell, J. Ruan, *et al.*, 2009 The Sequence Alignment/Map format and SAMtools. Bioinformatics 25: 2078–2079.

https://doi.org/10.1093/bioinformatics/btp352

Li H., 2011 A statistical framework for SNP calling, mutation discovery, association mapping and population genetical parameter estimation from sequencing data. Bioinformatics 27: 2987–2993. https://doi.org/10.1093/bioinformatics/btr509

Li D., C.-M. Liu, R. Luo, K. Sadakane, and T.-W. Lam, 2015 MEGAHIT: an ultra-fast single-node solution for large and complex metagenomics assembly via succinct de Bruijn graph. Bioinformatics 31: 1674–1676. https://doi.org/10.1093/bioinformatics/btv033

Li H., 2016 Minimap and miniasm: fast mapping and de novo assembly for noisy long sequences. Bioinformatics 32: 2103–2110. https://doi.org/10.1093/bioinformatics/btw152

Luo R., B. Liu, Y. Xie, Z. Li, W. Huang, *et al.*, 2012 SOAPdenovo2: an empirically improved memory-efficient short-read de novo assembler. GigaScience 1: 2047-217X-1–18. https://doi.org/10.1186/2047-217X-1-18

Lynch M., A. Seyfert, B. Eads, and E. Williams, 2008 Localization of the Genetic Determinants of Meiosis Suppression in Daphnia pulex. Genetics 180: 317–327. https://doi.org/10.1534/genetics.107.084657

Maccari M., A. Gómez, F. Hontoria, and F. Amat, 2013a Functional rare males in diploid parthenogenetic Artemia. J. Evol. Biol. 26: 1934–1948. https://doi.org/10.1111/jeb.12191

Maccari M., F. Amat, and A. Gómez, 2013b Origin and Genetic Diversity of Diploid Parthenogenetic Artemia in Eurasia. PLOS ONE 8: e83348. https://doi.org/10.1371/journal.pone.0083348

Maccari M., F. Amat, F. Hontoria, and A. Gómez, 2014 Laboratory generation of new parthenogenetic lineages supports contagious parthenogenesis in Artemia. PeerJ 2: e439. https://doi.org/10.7717/peerj.439

Mank J. E., 2013 Sex chromosome dosage compensation: definitely not for everyone. Trends Genet. 29: 677–683. https://doi.org/10.1016/j.tig.2013.07.005

Manni M., M. R. Berkeley, M. Seppey, F. A. Simão, and E. M. Zdobnov, 2021 BUSCO Update:

Novel and Streamlined Workflows along with Broader and Deeper Phylogenetic Coverage for Scoring of Eukaryotic, Prokaryotic, and Viral Genomes. Mol. Biol. Evol. 38: 4647–4654. https://doi.org/10.1093/molbev/msab199

Meiklejohn C. D., E. L. Landeen, J. M. Cook, S. B. Kingan, and D. C. Presgraves, 2011 Sex chromosome-specific regulation in the Drosophila male germline but little evidence for chromosomal dosage compensation or meiotic inactivation. PLoS Biol. 9: e1001126. https://doi.org/10.1371/journal.pbio.1001126

Mignerot L., K. Avia, R. Luthringer, A. P. Lipinska, A. F. Peters, *et al.*, 2019 A key role for sex chromosomes in the regulation of parthenogenesis in the brown alga Ectocarpus. PLoS Genet. 15: e1008211. https://doi.org/10.1371/journal.pgen.1008211

Mullon C., A. E. Wright, M. Reuter, A. Pomiankowski, and J. E. Mank, 2015 Evolution of dosage compensation under sexual selection differs between X and Z chromosomes. Nat. Commun. 6: 7720. https://doi.org/10.1038/ncomms8720

Neiman M., T. F. Sharbel, and T. Schwander, 2014 Genetic causes of transitions from sexual reproduction to asexuality in plants and animals. J. Evol. Biol. 27: 1346–1359. https://doi.org/10.1111/jeb.12357

Nougué O., N. O. Rode, R. Jabbour-Zahab, A. Ségard, L.-M. Chevin, *et al.*, 2015 Automixis in Artemia: solving a century-old controversy. J. Evol. Biol. 28: 2337–2348. https://doi.org/10.1111/jeb.12757

Palmer D. H., T. F. Rogers, R. Dean, and A. E. Wright, 2019 How to identify sex chromosomes and their turnover. Mol. Ecol. 28: 4709–4724. https://doi.org/10.1111/mec.15245

Parraguez M., G. Gajardo, and J. A. Beardmore, 2009 The New World Artemia species A. franciscana and A. persimilis are highly differentiated for chromosome size and heterochromatin content. Hereditas 146: 93–103. https://doi.org/10.1111/j.1601-5223.2009.02109.x

Pennell M. W., J. E. Mank, and C. L. Peichel, 2018 Transitions in sex determination and sex

887 chromosomes across vertebrate species. Mol. Ecol. 27: 3950–3963.
888 https://doi.org/10.1111/mec.14540
889 Picard M. A. L., C. Cosseau, S. Ferré, T. Quack, C. G. Grevelding, *et al.*, 2018 Evolution of
890 gene dosage on the Z-chromosome of schistosome parasites. eLife 7: e35684.
891 https://doi.org/10.7554/eLife.35684
892 Picard M. A. L., B. Vicoso, S. Bertrand, and H. Escriva, 2021 Diversity of Modes of
893 Reproduction and Sex Determination Systems in Invertebrates, and the Putative
894 Contribution of Genetic Conflict. Genes 12: 1136.
895 https://doi.org/10.3390/genes12081136
896 Ponnikas S., H. Sigeman, J. K. Abbott, and B. Hansson, 2018 Why Do Sex Chromosomes Stop
897 Recombining? Trends Genet. 34: 492–503. https://doi.org/10.1016/j.tig.2018.04.001
898 Robinson J. T., D. Turner, N. C. Durand, H. Thorvaldsdóttir, J. P. Mesirov, *et al.*, 2018
899 Juicebox.js Provides a Cloud-Based Visualization System for Hi-C Data. Cell Syst. 6:
900 256-258.e1. https://doi.org/10.1016/j.cels.2018.01.001
901 Rode N. O., R. Jabbour-Zahab, L. Boyer, É. Flaven, F. Hontoria, *et al.*, 2022 The origin of
902 asexual brine shrimps. Am. Nat. https://doi.org/10.1086/720268
903 Rosin L. F., D. Chen, Y. Chen, and E. P. Lei, 2022 Dosage compensation in Bombyx mori is
904 achieved by partial repression of both Z chromosomes in males. Proc. Natl. Acad. Sci.
905 119: e2113374119. https://doi.org/10.1073/pnas.2113374119
906 Rovatsos M., and L. Kratochvíl, 2021 Evolution of dosage compensation does not depend on
907 genomic background. Mol. Ecol. 30: 1836–1845. https://doi.org/10.1111/mec.15853
908 Ruan J., and H. Li, 2020 Fast and accurate long-read assembly with wtdbg2. Nat. Methods 17:
909 155–158. https://doi.org/10.1038/s41592-019-0669-3
910 Sainz-Escudero L., E. K. López-Estrada, P. C. Rodríguez-Flores, and M. García-París, 2021
911 Settling taxonomic and nomenclatural problems in brine shrimps, Artemia (Crustacea:
912 Branchiopoda: Anostraca), by integrating mitogenomics, marker discordances and

913 nomenclature rules. PeerJ 9: e10865. https://doi.org/10.7717/peerj.10865
914 Sandrock C., and C. Vorburger, 2011 Single-Locus Recessive Inheritance of Asexual
915 Reproduction in a Parasitoid Wasp. Curr. Biol. 21: 433–437.
916 https://doi.org/10.1016/j.cub.2011.01.070
917 Schwander T., and B. J. Crespi, 2009 Multiple direct transitions from sexual reproduction to
918 apomictic parthenogenesis in Timema stick insects. Evol. Int. J. Org. Evol. 63: 84–103.
919 https://doi.org/10.1111/j.1558-5646.2008.00524.x
920 Schwentner M., S. Richter, D. C. Rogers, and G. Giribet, 2018 Tetraconatan phylogeny with
921 special focus on Malacostraca and Branchiopoda: highlighting the strength of taxon-
922 specific matrices in phylogenomics. Proc. Biol. Sci. 285: 20181524.
923 https://doi.org/10.1098/rspb.2018.1524
924 Sigeman H., M. Strandh, E. Proux-Wéra, V. E. Kutschera, S. Ponnikas, *et al.*, 2021 Avian Neo-
925 Sex Chromosomes Reveal Dynamics of Recombination Suppression and W
926 Degeneration. Mol. Biol. Evol. 38: 5275–5291. https://doi.org/10.1093/molbev/msab277
927 Straub T., and P. B. Becker, 2007 Dosage compensation: the beginning and end of
928 generalization. Nat. Rev. Genet. 8: 47–57. https://doi.org/10.1038/nrg2013
929 Talavera G., and J. Castresana, 2007 Improvement of Phylogenies after Removing Divergent
930 and Ambiguously Aligned Blocks from Protein Sequence Alignments. Syst. Biol. 56:
931 564–577. https://doi.org/10.1080/10635150701472164
932 Toman J., and J. Flegr, 2018 General environmental heterogeneity as the explanation of
933 sexuality? Comparative study shows that ancient asexual taxa are associated with both
934 biotically and abiotically homogeneous environments. Ecol. Evol. 8: 973–991.
935 https://doi.org/10.1002/ece3.3716
936 Törönen P., A. Medlar, and L. Holm, 2018 PANNZER2: a rapid functional annotation web
937 server. Nucleic Acids Res. 46: W84–W88. https://doi.org/10.1093/nar/gky350
938 Turner S. D., 2018 qqman: an R package for visualizing GWAS results using Q-Q and

939 manhattan plots. J. Open Source Softw. 3: 731. https://doi.org/10.21105/joss.00731
940 Van Stappen G., 2002 Zoogeography, pp. 171–224 in *Artemia: Basic and Applied Biology*,
941 Biology of Aquatic Organisms. edited by Abatzopoulos Th. J., Beardmore J. A., Clegg J.
942 S., Sorgeloos P. Springer Netherlands, Dordrecht.
943 Vaser R., I. Sović, N. Nagarajan, and M. Šikić, 2017 Fast and accurate de novo genome
944 assembly from long uncorrected reads. Genome Res. 27: 737–746.
945 https://doi.org/10.1101/gr.214270.116
946 Vibranovski M. D., H. F. Lopes, T. L. Karr, and M. Long, 2009 Stage-Specific Expression
947 Profiling of Drosophila Spermatogenesis Suggests that Meiotic Sex Chromosome
948 Inactivation Drives Genomic Relocation of Testis-Expressed Genes. PLOS Genet. 5:
949 e1000731. https://doi.org/10.1371/journal.pgen.1000731
950 Vicoso B., and D. Bachtrog, 2009 Progress and prospects toward our understanding of the
951 evolution of dosage compensation. Chromosome Res. 17: 585.
952 https://doi.org/10.1007/s10577-009-9053-y
953 Vicoso B., J. J. Emerson, Y. Zektser, S. Mahajan, and D. Bachtrog, 2013 Comparative sex
954 chromosome genomics in snakes: differentiation, evolutionary strata, and lack of global
955 dosage compensation. PLoS Biol. 11: e1001643.
956 https://doi.org/10.1371/journal.pbio.1001643
957 Vicoso B., 2019 Molecular and evolutionary dynamics of animal sex-chromosome turnover. Nat.
958 Ecol. Evol. 3: 1632–1641. https://doi.org/10.1038/s41559-019-1050-8
959 Walters J. R., and T. J. Hardcastle, 2011 Getting a full dose? Reconsidering sex chromosome
960 dosage compensation in the silkworm, Bombyx mori. Genome Biol. Evol. 3: 491–504.
961 https://doi.org/10.1093/gbe/evr036
962 Wang M., and L. Kong, 2019 pblat: a multithread blat algorithm speeding up aligning sequences
963 to genomes. BMC Bioinformatics 20: 28. https://doi.org/10.1186/s12859-019-2597-8
964 Willforss J., A. Chawade, and F. Levander, 2019 NormalyzerDE: Online Tool for Improved

Normalization of Omics Expression Data and High-Sensitivity Differential Expression Analysis. J. Proteome Res. 18: 732–740. https://doi.org/10.1021/acs.jproteome.8b00523

Wright A. E., R. Dean, F. Zimmer, and J. E. Mank, 2016 How to make a sex chromosome. Nat. Commun. 7: 12087. https://doi.org/10.1038/ncomms12087

Yagound B., K. A. Dogantzis, A. Zayed, J. Lim, P. Broekhuyse, *et al.*, 2020 A Single Gene Causes Thelytokous Parthenogenesis, the Defining Feature of the Cape Honeybee Apis mellifera capensis. Curr. Biol. 30: 2248-2259.e6. https://doi.org/10.1016/j.cub.2020.04.033

Zeileis A., and G. Grothendieck, 2005 zoo: S3 Infrastructure for Regular and Irregular Time Series. J. Stat. Softw. 14: 1–27. https://doi.org/10.18637/jss.v014.i06

Zhou Q., J. Zhang, D. Bachtrog, N. An, Q. Huang, *et al.*, 2014 Complex evolutionary trajectories of sex chromosomes across bird taxa. Science 346: 1246338. https://doi.org/10.1126/science.1246338

Zhou C., S. A. McCarthy, and R. Durbin, 2022 YaHS: yet another Hi-C scaffolding tool. bioRxiv 2022.06.09.495093; doi: https://doi.org/10.1101/2022.06.09.495093

Figure 1: A shared sex-linked region on the ZW pair. A. Patterns of female/male coverage in *A. franciscana* and *A. sinica*. A rolling median of 20 windows (of 10KB each) is shown in red for *A. sinica*, and a rolling median of 5 scaffolds is shown in blue for *A. franciscana*. The light pink shaded area highlights the region between the 5th and 95th-percentiles of the rolling median of coverage for autosomes of *A. sinica*. The horizontal gray line at -1 signifies the expected twofold reduction in coverage in females compared to males of fully differentiated regions. The inferred differentiated regions of *A. sinica* are highlighted in gray, and the putative strata are defined above, along with the putative pseudoautosomal region (PAR). The red dots are the locations of the W-candidates shared between *A. sinica* and *A. franciscana*. B. Male:female F_{ST} along the putative chromosome Z. The dots are F_{ST} calculated for 1kb bins, and the black line is the rolling median computed in sliding windows of 30 consecutive 1000 nucleotide bins. The light blue shaded area highlights the region between the 5th and 95th-percentiles of the rolling median of F_{ST} for autosomes. C. Phylogenetic trees for two examples of the W-candidates shared between *A. sinica* and *A. franciscana* (red dots in panel A) and their putative Z homologs. *Branchinecta lindahli* is used as the outgroup.

Figure 2. Dosage compensation of the Z-chromosome. A: The log-transformed ratio of female to male expression along the Z chromosome in heads, gonads and thoraces (computed as the rolling median in sliding windows of 30 consecutive genes). Gray areas represent the differentiated regions identified in the coverage analysis, and the putative strata are denoted above, along with the putative pseudoautosomal region (PAR).The dashed horizontal black line is at zero. B-D: The distribution of log-transformed ratio of female to male expression for the autosomes and the different regions of the Z chromosome in thoraces (A), heads (B) and gonads (C). The number of genes in each of the different regions is indicated underneath the x-axis labels. A wilcoxon rank sum test was used to assess the significance of the difference between the expression of the autosomes and the different regions of the Z chromosome, with a Bonferroni correction for the four comparisons performed in each tissue. *** denotes a p-value <=0.001.

Figure 3: The sex chromosomes of sexual and asexual individuals. A. Coverage patterns in *A. sp. Kazakhstan* male and female samples, in three asexual females, and in a rare male derived from an asexual lineage from Aibi Lake. Areas shaded in gray represent the differentiated regions of the *A. sinica* ZW pair. B. The fraction of SNPs that lost heterozygosity on the rare male Z chromosome relative to its asexual sister in bins of 500Kb. The dotted line represents the average loss of heterozygosity for autosomes.

Figure 4. Elevated F_{ST} between sexual and asexual females localizes to the Z chromosome. A. Manhattan plot of F_{ST} estimated for 1Kb sliding windows between asexual and sexual females across the genome. B. F_{ST} across chromosome 1. F_{ST} is shown for individual SNPs in light green, and the blue line shows the rolling median for 101 SNPs. Areas shaded in gray represent the differentiated regions of the *A. sinica* ZW pair.

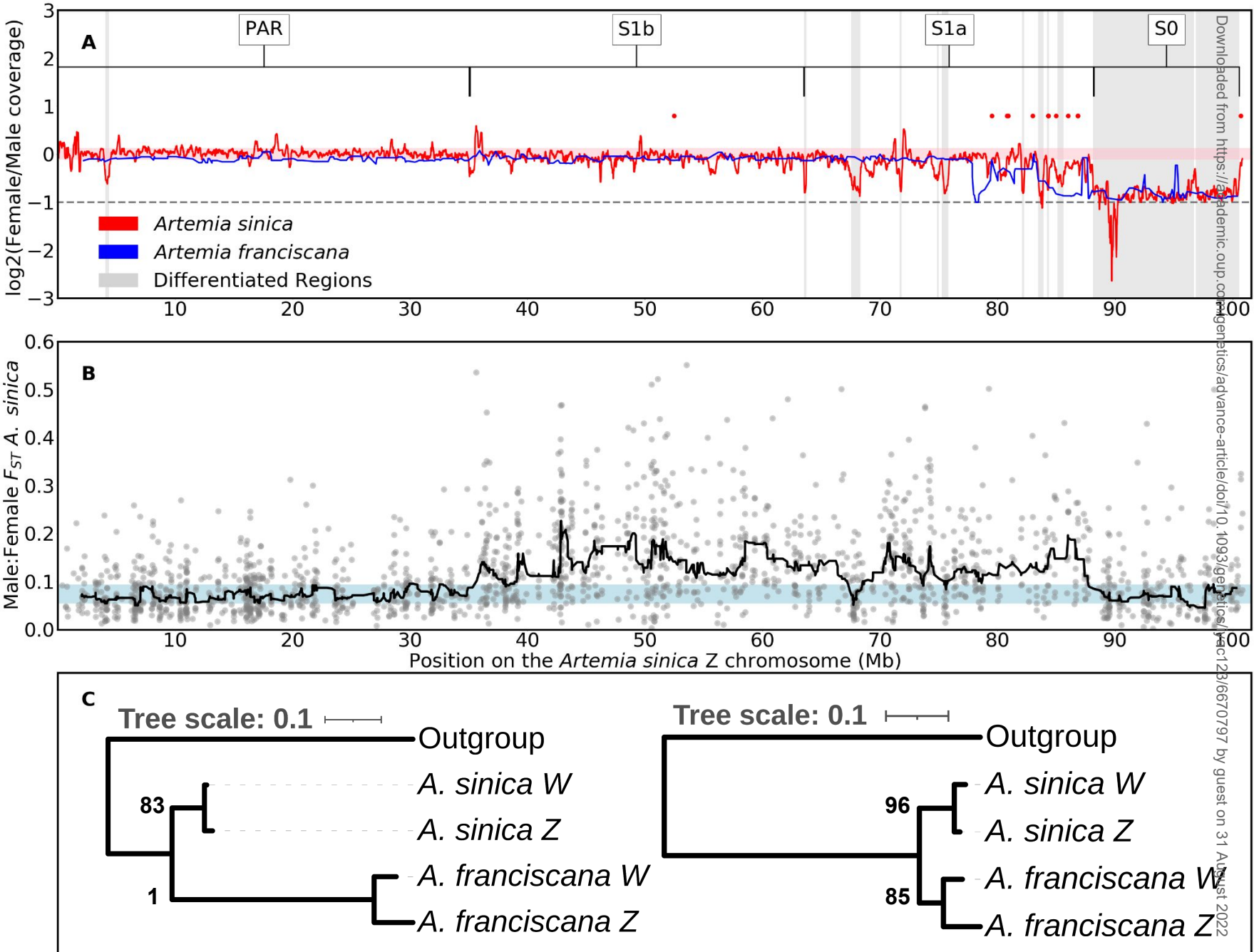

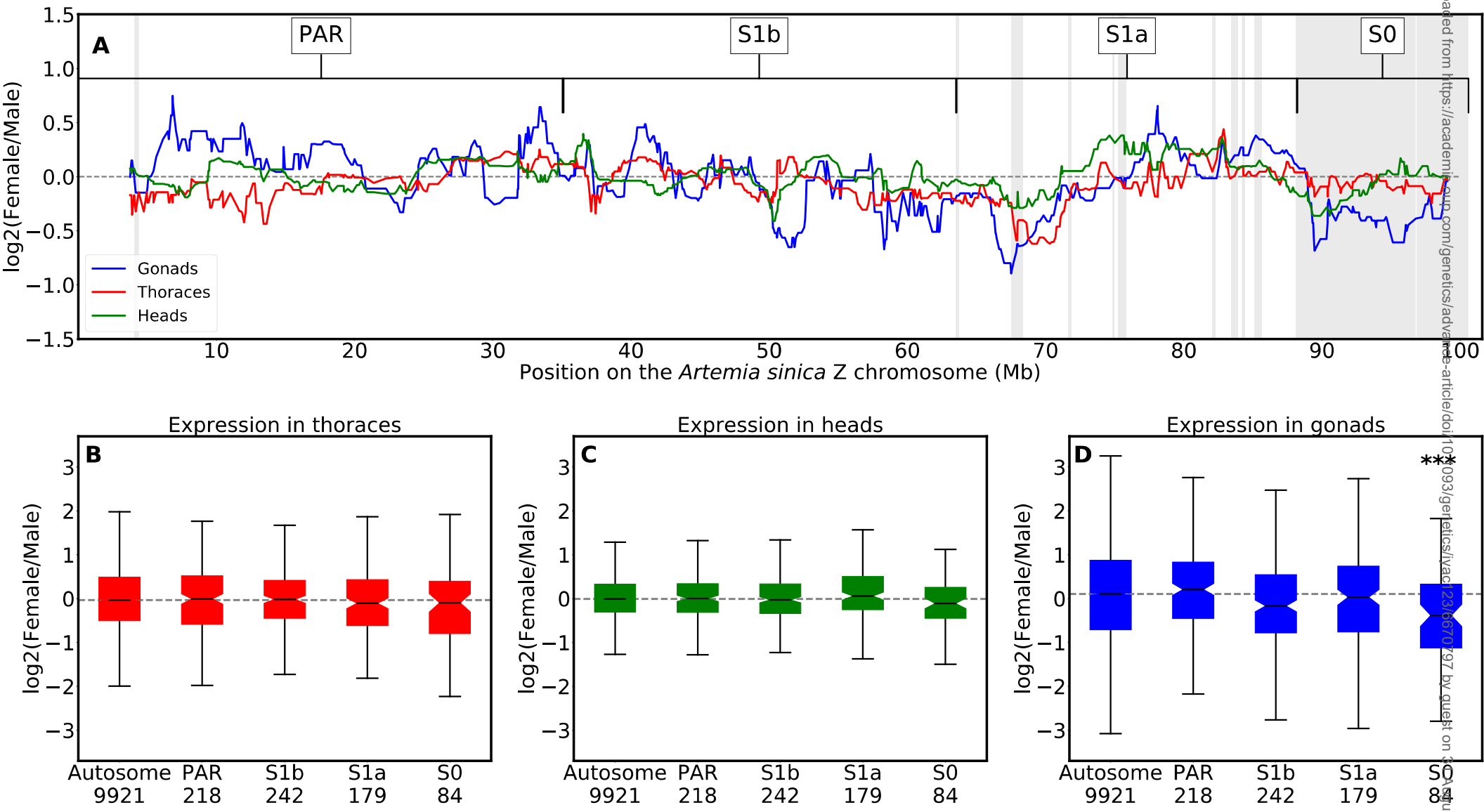

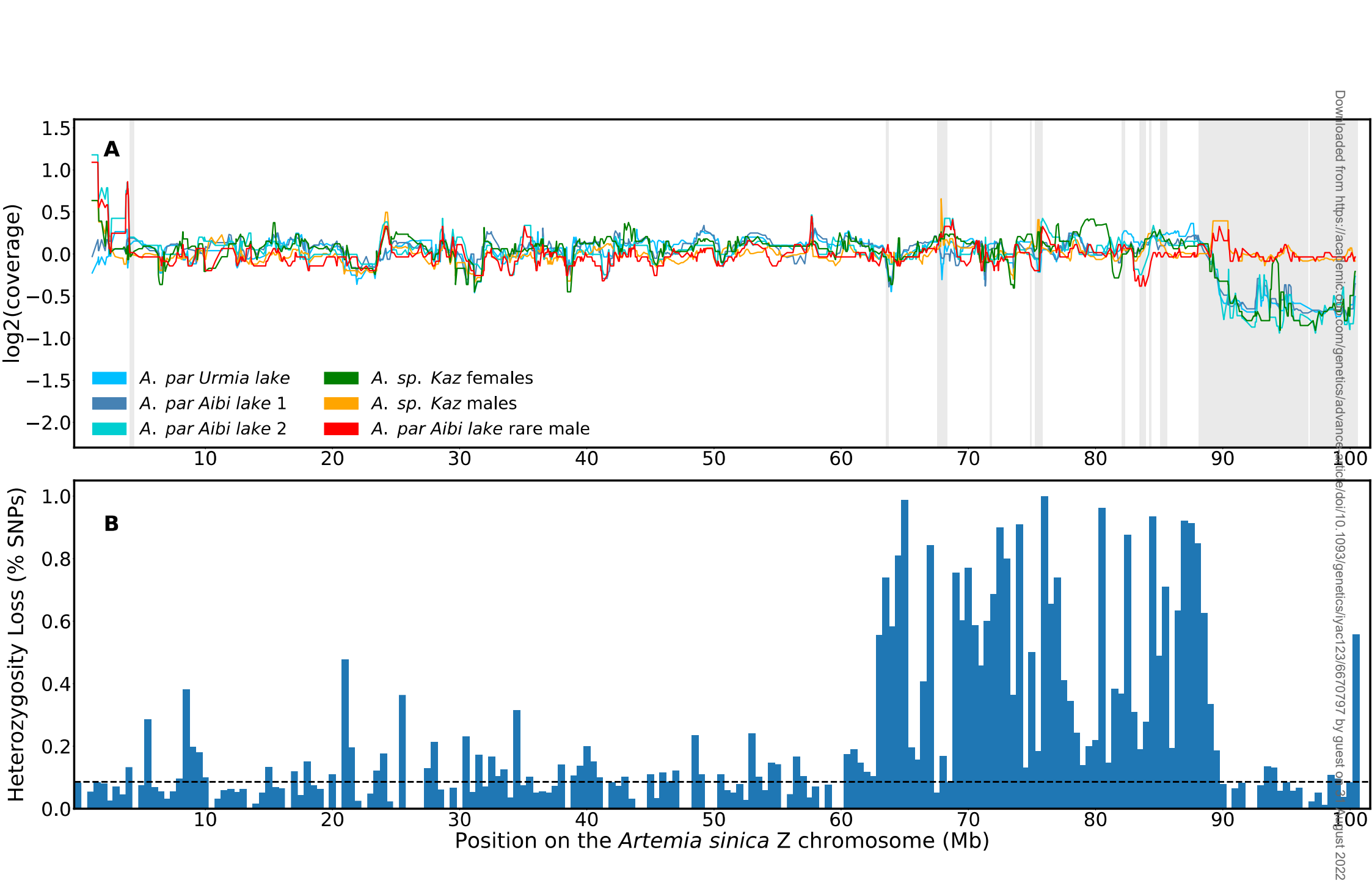

A

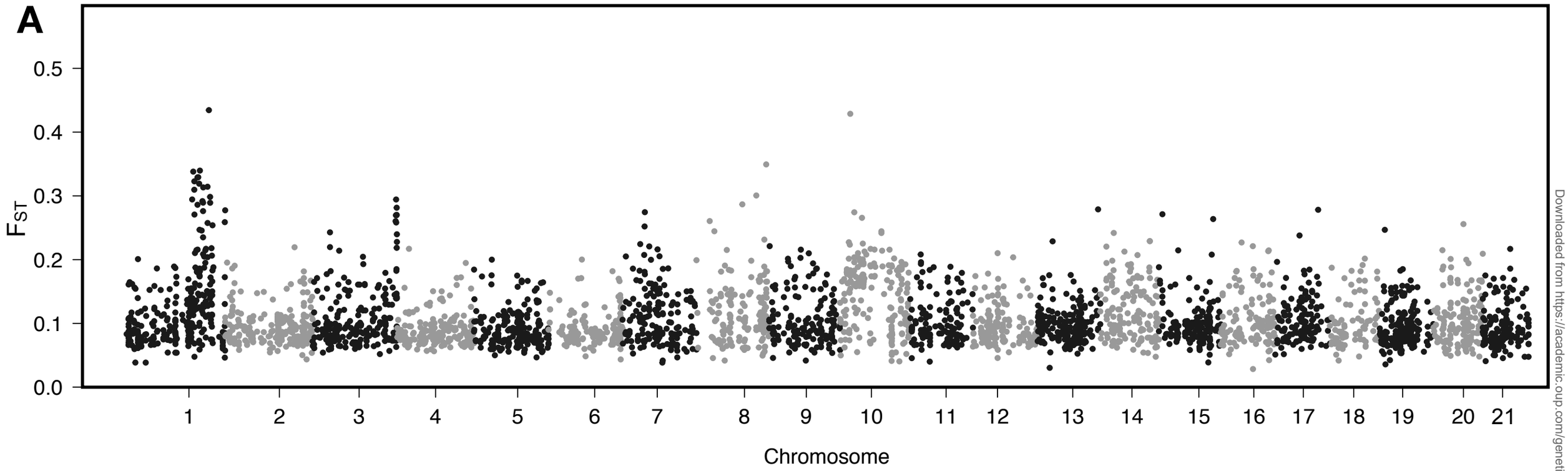

B